PNAS
www.pnas.org

Supplementary Information for

Bumblebees perceive the spatial layout of their environment in relation to their body size and form to minimize inflight collisions

Sridhar Ravi[1&2*], Tim Siesenop[1], Olivier Bertrand[1], Liang Li[3], Charlotte Dousott[1], William Warren[4], Stacey Combes[5] and Martin Egelhaaf[1]

*Sridhar Ravi
Email: Sridhar.ravi@adfa.edu.au

This PDF file includes:

- Supplementary text
- Figures S1 to S7
- Tables S1 to S11
- Legends for Movies S1 to S7
- Legend for Dataset
- SI References

Other supplementary materials for this manuscript include the following:

- Movies S1 to S7

www.pnas.org/cgi/doi/10.1073/pnas.2016872117

Estimation of gap-size by peering

Prior studies on bees and other insects have revealed that bees use optic flow for flight stabilization and control, and use spatial and temporal variations in optic flow for edge identification (1, 2), depth and gap perception (3–5). We hypothesize a simpler mechanism by which bees could determine the spatial properties of a gap (gap size) based on the peering motions they perform (Fig. 1 & S3). Assuming that bees are capable of identifying the edge of the gap(6) and monitoring the optic flow induced by the gap edges during peering motions, gap size could be obtained as follows:

Bees produce oscillating lateral motions by directing the aerodynamic force in the lateral direction through rotation of the body along the longitudinal axis (i.e. body roll) (7–9). It is known that for small roll angles, the bee's lateral acceleration (a) is directly proportional to its roll angle (ρ) (9, 10):

$$a = g\rho \qquad (1)$$

Where g is the acceleration due to gravity, see Fig. S6.

For smaller apertures the bees tended to reduce their forward velocity in the vicinity of the gap and mainly engaged in lateral manoeuvring in front of the gaps' edges, Fig. 1&2. Therefore, neglecting the forward flight and considering a peering pass that consists of steady lateral acceleration from rest, for a given instantaneous roll angle, the bee's lateral velocity (V) is directly proportional to the elapsed time (t), from Equ. 1:

$$V = at \text{ or } V = g\rho t \qquad (2)$$

Bees mainly use monocular vision and their eyes can be approximated as a sphere and the retina as a point – a similar approach has been used in numerous previous studies (11–13). The general equation for the true optic flow of an arbitrary point ($\dot{\beta}$) due to the velocity of the bee (Fig. S6) can be expressed following the expression in (14):

$$\dot{\beta} = \frac{V sin\beta}{d} \qquad (3)$$

Where β is the visual angle between the direction of flight and the direction to the point in space, *d* is the distance to the point, and $\dot{\beta}$ is the optical velocity of the point (Fig. S6). See (15) for elaboration on optic flow.

Rearranging Equ. 3, the distance between the bee and the point can be expressed as:

$$d = \frac{V sin\beta}{\dot{\beta}} \qquad (4)$$

Considering Fig. S6, using Equ. 4 the distances between the bee and the left and right edges of the gap can be expressed as:

$$d_L = \frac{V sin\beta_L}{\dot{\beta}_L} \qquad d_R = \frac{V sin\beta_R}{\dot{\beta}_R} \qquad (5)$$

The widths of left and right parts of the gap (Fig. S6) are:

$$G_L = d_L sin\alpha_L \qquad G_R = d_R sin\alpha_R \qquad (6)$$

And the total gap width is given by

$$G = G_L + G_R \qquad (7)$$

Substituting Equ. 5 & 6 into 7:

$$G = V\left(\frac{sin\beta_L sin\alpha_L}{\dot{\beta}_L} + \frac{sin\beta_R sin\alpha_R}{\dot{\beta}_R}\right) \qquad (8)$$

Expressing the velocity of the bee (V) in terms of the body roll angle by substituting Equ. 2 into 8

$$G = g\rho t\left(\frac{sin\beta_L sin\alpha_L}{\dot{\beta}_L} + \frac{sin\beta_R sin\alpha_R}{\dot{\beta}_R}\right) \qquad (9)$$

α can be eliminated as follows from Fig. S6:

$$\alpha_L = -(90^\circ - \beta_L) \qquad (10)$$

$$sin\alpha_L = sin[-(90^\circ - \beta_L)] = cos(-\beta_L) = cos\beta_L \qquad (11)$$

$$\alpha_R = 90^\circ - \beta_R \qquad (12)$$

$$sin\alpha_R = sin(90^\circ - \beta_R) = cos\beta_L \qquad (13)$$

Substituting Equ. 11 & 13 into 9 yields the following simplified equation:

$$G = g\rho t\left(\frac{sin\beta_L cos\beta_L}{\dot{\beta}_L} + \frac{sin\beta_R cos\beta_R}{\dot{\beta}_R}\right) \quad (14)$$

Thus, the absolute gap width is specified by the optical velocities of the left and right edges ($\dot{\beta}$) and the visual directions of the left and right edges relative to the flight direction (β), scaled by the bee's roll angle (ρ) and elapsed time (t) during the lateral maneuvers. Gap width is given in the same length unit as a and V, which might be calibrated during development as wingspans/sec. Thus, gap width would be scaled to wingspans.

In order to employ this method of gap-size estimation during lateral peering, bees must be able to perceive the optic flow and angular position of either edge of the gap on their retina, and must also encode their instantaneous body roll angle (ρ). While limited direct evidence exists of bees encoding their body orientation for spatial perception, insects stabilize their head during voluntary manoeuvres by performing coordinated counter rotations with respect to the body (16–18). This behaviour suggests that insects indeed possess the capacity to measure and monitor the relative angular position of the head and body. Further research to test whether bees indeed use a combination of optic flow and ego motion estimation for spatial perception will be useful.

This derived method relies on using body roll as a proxy for lateral acceleration (i.e. ego motion) and could explain the following behaviors displayed by the bees: lateral acceleration produced by body roll is insensitive to body size and therefore big and small bees need to perform similar maneuvers to estimate gap size. The peering amplitude of the bees was found to be bodysize insensitive for all gap-sizes presented. The method presented here relies on lateral maneuvers being performed within the edges of the gaps. For all gap-sizes, the peering motion was mainly between the edges of the gap and the mean peering amplitude was smaller than gap width.

Supplementary Figures

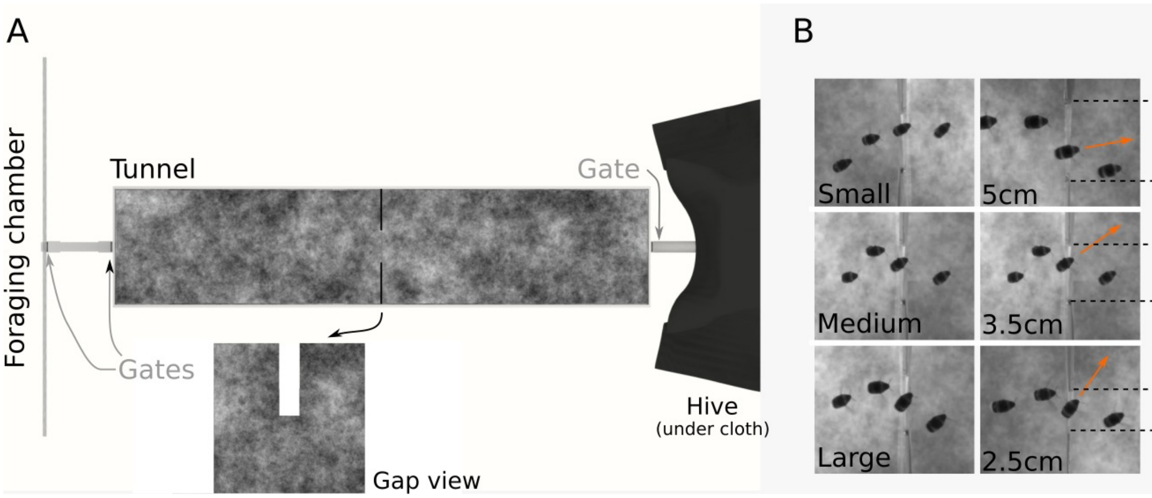

Figure S1: (a) Schematic of experimental setup presented from top-view, see SV1 for animated rendering of experiment setup. (b) Snapshot of bees of different sizes passing through gaps of varying widths. (1) Ws = 22mm, Gs = 40mm, Yaw = 29° (2) Ws = 26mm, Gs = 40mm, Yaw = 40° (3) Ws = 31mm, Gs = 40mm, Yaw = 66° (4) Ws = 31mm, Gs = 50mm, Yaw = 8° (5) Ws = 26mm, Gs = 35mm, Yaw = 31° (6) Ws = 28mm, Gs = 25mm, Yaw = 78°

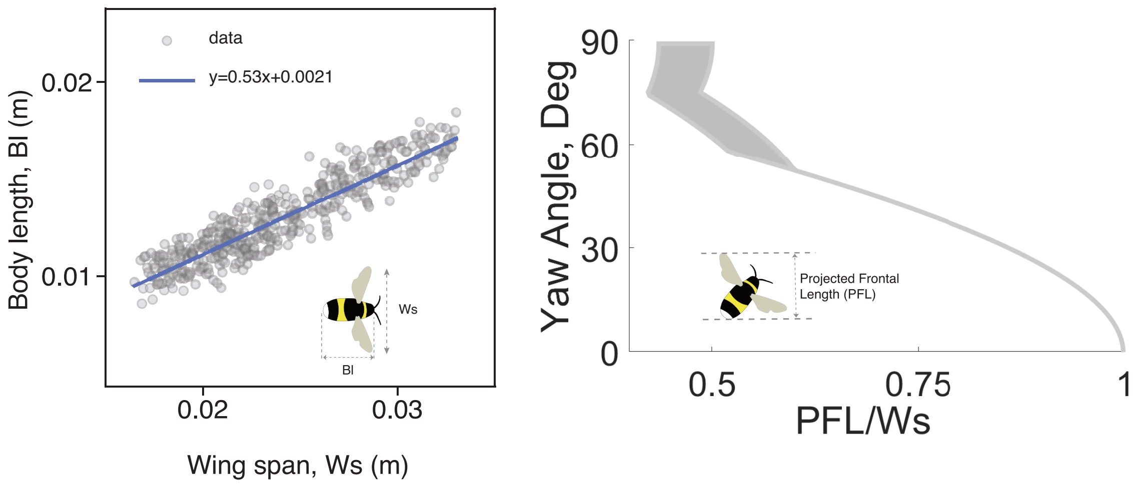

Figure S2: (a) Scatter representation of the wingspan and body length of bees during steady level flight with a linear fit relating the two morphological properties (n=400), R-squared = 0.89. (b) The projected frontal length (PFL) of all bees normalized with respect to wingspan for different yaw/heading angles.

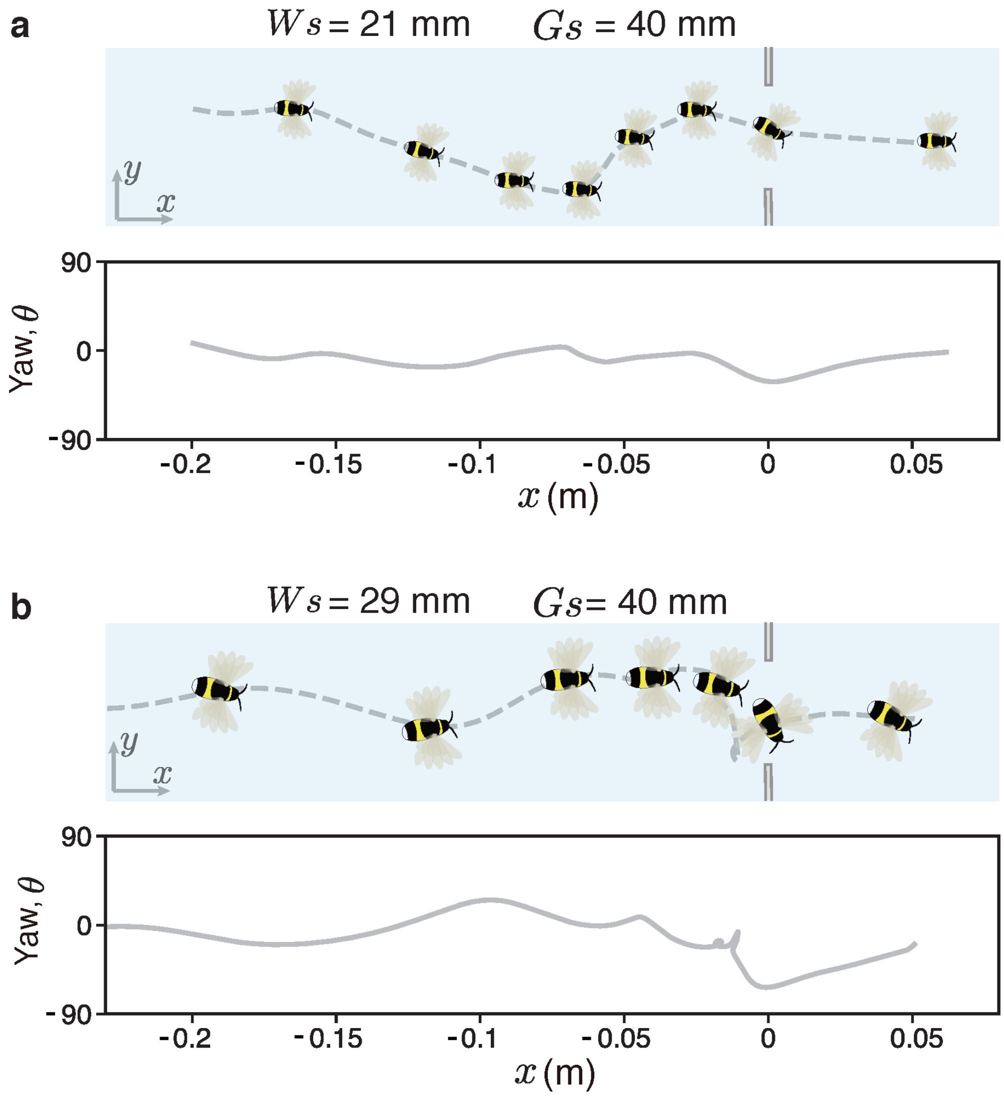

Figure S3: Sample flight trajectory of bees with Ws = 21 and 29mm (a & b) respectively flying through 40mm wide gap. Instantaneous yaw angle of the bees for each flight trajectory is also plotted

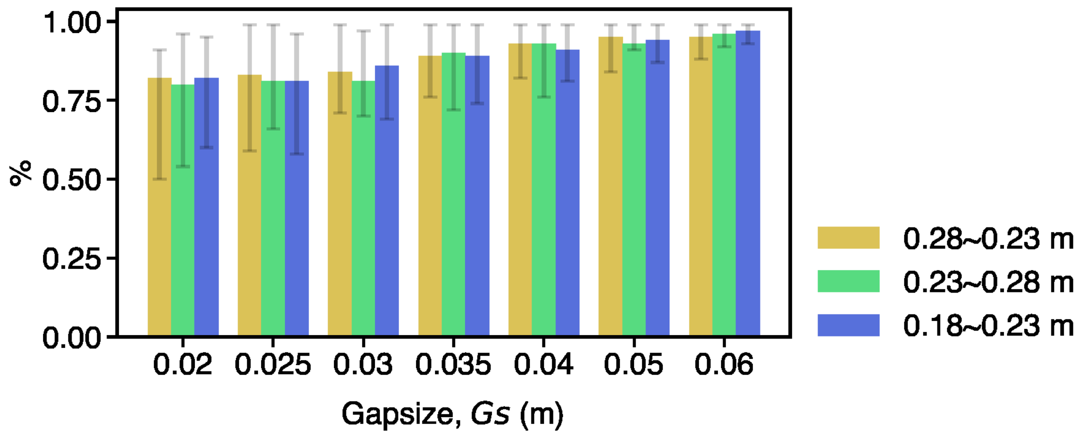

Figure S4: The proportion of time while the bees were in the vicinity of the gaps that any part of the gap or its edges was within 60Deg of their visual field. The mean, 5^{th} and 95^{th} percentiles are included. The vicinity of the gap is characterized as a 100mm square region placed 5mm from the edge of the gap. Majority of peering occurred within this region for all gaps. The region within 5mm to the gap was excluded as reorienting behaviour was initiated in this region for narrow gaps. The number of flights recorded, contacts and collisions for different gap sizes for bees with different wingspans are given in Supplementary Table S1.

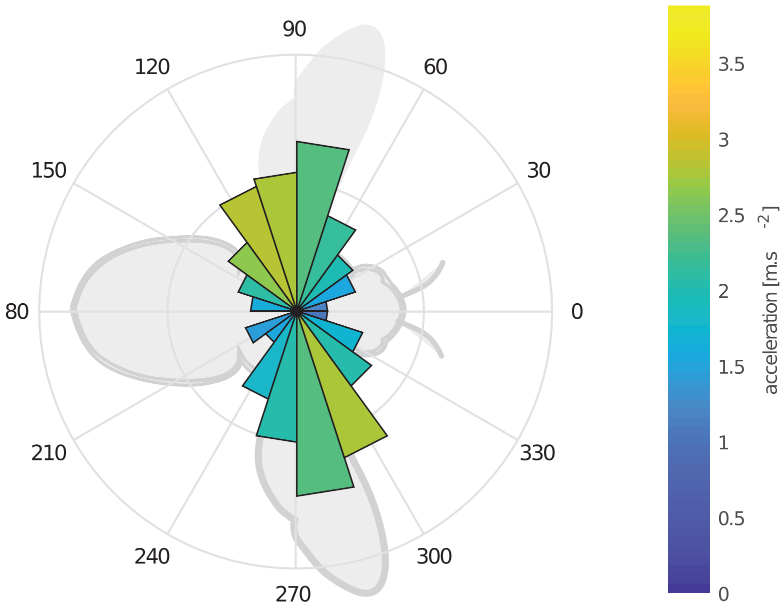

Figure S5: Representative rose plot of a bee’s acceleration during peering when the gapsize = 25mm. The bee’s wingspan = 22mm

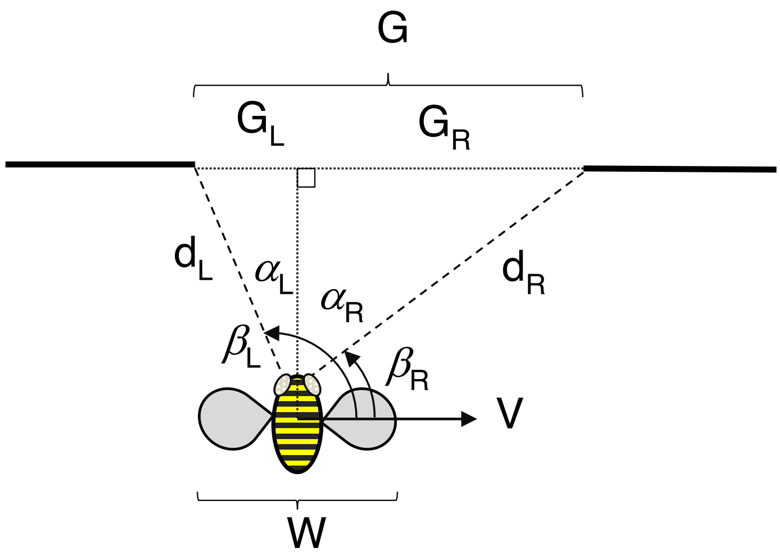

Figure S6: Schematic of the bee flying near the gap performing lateral manoeuvres between the gap's edges. G = gapsize, G_r and G_l is the distance between the bee's lateral position and the right and left edges of the gap respectively. d_r and d_l is the vector distance between the bee's retina and the left and right edges of the gap respectively. β_L and β_L is the angle between the bees' velocity vector and the vector connecting the bee's retina and the left and right edges of the gap respectively. β_L and β_L is the angle between the bees' velocity vector and the vector connecting the bee's retina and the left and right edges of the gap respectively.

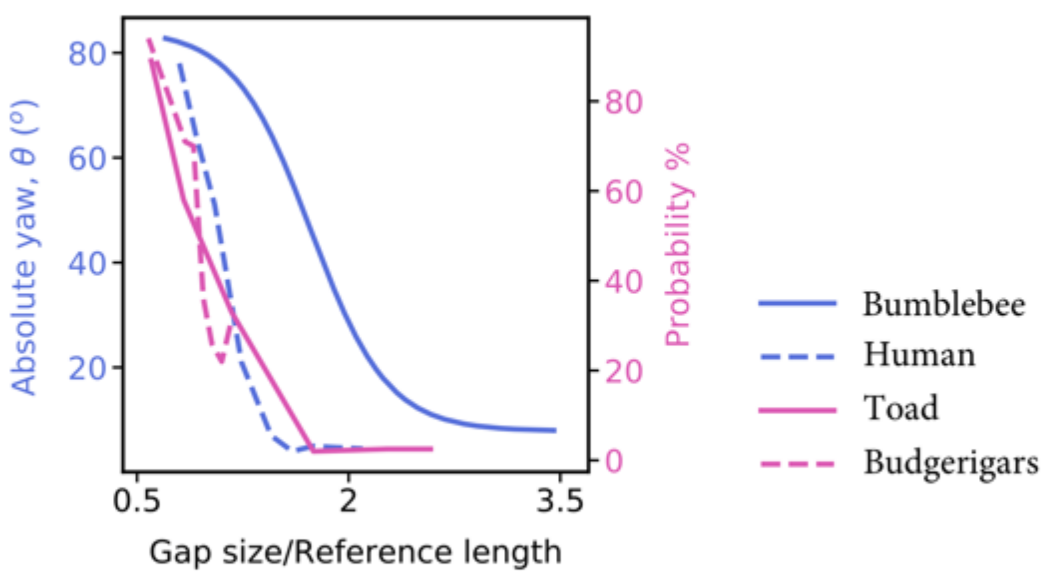

Figure S7: Absolute yaw angle of bumblebees and shoulder rotation of humans while passing through different gap. Gap size is normalized against the wingspan for bees while it was normalized with shoulder width in humans. Data on bumblebees from present study, sigmoidal relationship from Fig. 3b of main text. Data on humans from Fig. 1 in (19). The probability of wing tuck for budgerigars flying through gaps of different sizes that is normalized against their wingspan, data from Fig. 3 in (20) & mean wingspan = 30cm. The probability toads to detour around gaps of different sizes that is normalized against their head width, data from Fig. 2 in (21) and head width = 3cm.

Supplementary Tables

Wingspan Groups (mm)	Gapsize Treatment (mm)						
	20 (T1)	**25 (T2)**	**30 (T3)**	**35 (T4)**	**40 (T5)**	**50 (T6)**	**60 (T7)**
18-23 (G1)	19,8,4	20,8,4	20,8,2	20,4,0	20,3,0	17,0,0	18,0,0
23-28 (G2)	20,11,9	19,10,6	20,9,6	20,4,0	18,3,0	18,2,0	18,0,0
28-33 (G3)	17,13,11	19,12,8	20,11,8	20,6,2	19,6,0	19,2,0	19,0,0

Table S1: Table showing the total number of flights recorded, contacts and collisions for bees of different wingspans and gaps sizes. The first number in the cell represents to total number of flights recorded for bees in that wingspan range and gap size combination while the second number represents number of flights where bees made contact with the obstacle and the last number represents number of flights where wing collisions occurred.

Gapsize Treatment	Wingspan Group	Wingspan Group	Adjusted p-value	Significance (Adjusted)
T1	G1	G2	0.06	ns
T1	G1	G3	0.84	ns
T1	G2	G3	0.525	ns
T2	G1	G2	0.621	ns
T2	G1	G3	1	ns
T2	G2	G3	0.432	ns
T3	G1	G2	0.873	ns
T3	G1	G3	1	ns
T3	G2	G3	1	ns
T4	G1	G2	1	ns
T4	G1	G3	1	ns
T4	G2	G3	1	ns
T5	G1	G2	1	ns
T5	G1	G3	1	ns
T5	G2	G3	1	ns
T6	G1	G2	1	ns
T6	G1	G3	1	ns
T6	G2	G3	1	ns
T7	G1	G2	0.219	ns
T7	G1	G3	1	ns
T7	G2	G3	0.996	ns

Table S2: Results of ANOVA tests for the peering amplitude of the bees of different wingspan groups for the different gaps (Figure 2a). Details on Wingspan groups and Gapsize treatments is indicated in Table S1.

Wingspan Group	Gapsize Treatment	Variable	Statistic	p-value
G1	T1	score	0.9260	0.1462
G2	T1	score	0.9786	0.9142
G3	T1	score	0.9569	0.5739
G1	T2	score	0.9137	0.0751
G2	T2	score	0.9565	0.5057
G3	T2	score	0.9019	0.0527
G1	T3	score	0.9286	0.1451
G2	T3	score	0.9686	0.7256
G3	T3	score	0.9391	0.2302
G1	T4	score	0.9485	0.3443
G2	T4	score	0.9522	0.4018
G3	T4	score	0.9372	0.2122
G1	T5	score	0.9521	0.4004
G2	T5	score	0.9599	0.5996
G3	T5	score	0.9505	0.4034
G1	T6	score	0.9736	0.8784
G2	T6	score	0.8775	0.0237
G3	T6	score	0.9242	0.1352
G1	T7	score	0.9434	0.3306
G2	T7	score	0.8595	0.0120
G3	T7	score	0.9278	0.1576

Table S3. Results of data normality test for the peering amplitude of the bees of different wingspan groups for the different gaps (Figure 2a). Details on Wingspan groups and Gapsize treatments is indicated in Table S1.

Wingspan Group	Effect	DFd	F	p	p<.05	ges	Adjusted p-value
G1	Gapsize Treatments	6	96	62.631	5.06e-31	*	0.765
G2	Gapsize Treatments	6	102	53.358	2.78e-29	*	0.734
G3	Gapsize Treatments	6	96	63.92	2.34e-31	*	0.758

Table S4: Results of group ANOVA test for the peering amplitude of the bees of different wingspan groups for the different gaps (Figure 2a). Details on Wingspan groups and Gapsize treatments is indicated in Table S1.

Gapsize Treatment	Wingspan Group	Wingspan Group	Adjusted p-value	Significance (Adjusted)
T1	G1	G2	0.011	*
T1	G1	G3	3.9e-05	****
T1	G2	G3	0.66	ns
T2	G1	G2	0.051	ns
T2	G1	G3	0.001	**
T2	G2	G3	0.185	ns
T3	G1	G2	1	ns
T3	G1	G3	0.012	*
T3	G2	G3	0.000663	***
T4	G1	G2	0.024	*
T4	G1	G3	0.001	**
T4	G2	G3	0.369	ns
T5	G1	G2	0.732	ns
T5	G1	G3	0.000128	***
T5	G2	G3	0.005	**
T6	G1	G2	0.708	ns
T6	G1	G3	0.936	ns
T6	G2	G3	0.006	**
T7	G1	G2	0.107	ns
T7	G1	G3	1	ns
T7	G2	G3	0.612	ns

Table S5: Results of ANOVA tests for the mean number of peering passes performed by bees of different wingspan groups for the different gap treatments (Figure 2b). Details on Wingspan groups and Gapsize treatments is indicated in Table S1.

Wingspan Group	Gapsize Treatment	Variable	Statistic	p
G1	T1	score	0.9359	0.2218
G2	T1	score	0.9606	0.5569
G3	T1	score	0.9106	0.1024
G1	T2	score	0.9596	0.5352
G2	T2	score	0.9372	0.2344
G3	T2	score	0.9452	0.3260
G1	T3	score	0.9533	0.4199
G2	T3	score	0.9237	0.1168
G3	T3	score	0.8902	0.0272
G1	T4	score	0.9148	0.0788
G2	T4	score	0.9347	0.1902
G3	T4	score	0.9187	0.0934
G1	T5	score	0.9412	0.2527
G2	T5	score	0.9463	0.3693
G3	T5	score	0.8652	0.0120
G1	T6	score	0.9240	0.1723
G2	T6	score	0.9150	0.1055
G3	T6	score	0.9352	0.2157
G1	T7	score	0.9253	0.1607
G2	T7	score	0.9649	0.6986
G3	T7	score	0.9542	0.4647

Table S6. Results of data normality test for the mean number of peering passes performed by bees of different wingspan groups for the different gap treatments (Figure 2b). Details on Wingspan groups and Gapsize treatments is indicated in Table S1.

Wingspan Group	Effect	DFd	F	p	p<.05	ges	Adjusted p-value
G1	Gapsize Treatments	49.11	52.812	1.54e-15	*	0.744	4.62e-15
G2	Gapsize Treatments	49.49	44.611	6.23e-14	*	0.688	1.869e-13
G3	Gapsize Treatments	53.59	27.13	2.22e-11	*	0.612	6.66e-11

Table S7: Results of group ANOVA test for the mean number of peering passes performed by bees of different wingspan groups for the different gap treatments (Figure 2b). Details on Wingspan groups and Gapsize treatments is indicated in Table S1.

Gapsize Treatment	Wingspan Group	Wingspan Group	Unadjusted p-value	Significance (Unadjusted)	Adjusted p-value	Significance (Adjusted)
T1	G1	G2	0.787	ns	1	ns
T1	G1	G3	0.996	ns	1	ns
T1	G2	G3	0.799	ns	1	ns
T2	G1	G2	0.281	ns	0.844	ns
T2	G1	G3	9.85e-05	****	0.000296	***
T2	G2	G3	0.00262	**	0.00787	**
T3	G1	G2	0.0441	*	0.132	ns
T3	G1	G3	2.75e-05	****	8.24e-05	****
T3	G2	G3	0.0315	*	0.0944	ns
T4	G1	G2	4.32e-06	****	1.3e-05	****
T4	G1	G3	6.99e-11	****	2.1e-10	****
T4	G2	G3	0.000736	***	0.00221	**
T5	G1	G2	7.09e-05	****	0.000213	***
T5	G1	G3	5.02e-10	****	1.51e-09	****
T5	G2	G3	0.00192	**	0.00576	**
T6	G1	G2	0.0263	*	0.0788	ns
T6	G1	G3	6.42e-14	****	1.92e-13	****
T6	G2	G3	1.18e-08	****	3.53e-08	****
T7	G1	G2	0.00161	**	0.00482	**
T7	G1	G3	0.000505	***	0.00152	**
T7	G2	G3	0.541	ns	1	ns

Table S8: Results of ANOVA tests for the yaw angle of the bees of different wingspan groups as they passed through the different gap treatments (Figure 3a). Details on Wingspan groups and Gapsize treatments is indicated in Table S1.

Wingspan Group	Gapsize Treatment	Outlier ID	Score	Outlier	Extreme outlier
G3	T2	P1	67.11	TRUE	FALSE
G2	T3	P27	90	TRUE	FALSE
G2	T4	P1	27,515	TRUE	FALSE
G3	T4	P16	88,322	TRUE	FALSE
G3	T4	P17	90	TRUE	FALSE
G1	T5	P27	69,428	TRUE	FALSE
G1	T5	P28	70,343	TRUE	FALSE
G3	T5	P1	97,278	TRUE	TRUE
G3	T5	P2	13,923	TRUE	TRUE
G1	T7	P30	40,799	TRUE	FALSE
G1	T7	P31	42,078	TRUE	TRUE

Table S9: Results of outlier test for the yaw angle of the bees of different wingspan groups as they passed through the different gap treatments (Figure 3a). Details on Wingspan groups and Gapsize treatments is indicated in Table S1.

Wingspan Group	Gapsize Treatment	Variable	Statistic	p
G1	T1	score	0.9435	0.1031
G2	T1	score	0.9305	0.0635
G3	T1	score	0.9438	0.1658
G1	T2	score	0.9420	0.0405
G2	T2	score	0.9747	0.5513
G3	T2	score	0.9658	0.6136
G1	T3	score	0.9756	0.4672
G2	T3	score	0.9484	0.1961
G3	T3	score	0.9405	0.1524
G1	T4	score	0.9658	0.4121
G2	T4	score	0.9673	0.1890
G3	T4	score	0.8645	0.0041
G1	T5	score	0.8762	0.0033
G2	T5	score	0.9720	0.4841
G3	T5	score	0.7339	6.70E+08
G1	T6	score	0.9635	0.1858
G2	T6	score	0.9691	0.3832
G3	T6	score	0.9746	0.5998
G1	T7	score	0.8367	0.0003
G2	T7	score	0.9796	0.7037
G3	T7	score	0.9594	0.3381

Table S10. Results of data normality test for the yaw angle of the bees of different wingspan groups as they passed through the different gap treatments (Figure 3a). Details on Wingspan groups and Gapsize treatments is indicated in Table S1.

Wingspan Group	Effect	DFd	F	p	p<.05	ges	Adjusted p-value
G1	Gapsize Treatments	35.4	1,135,923	3.2e-30	*	0.876	9.6e-30
G2	Gapsize Treatments	79.68	3,136,643	6.79e-83	*	0.886	2.04E-79
G3	Gapsize Treatments	55.81	445.04	8.99e-38	*	0.86	2.70E-34

Table S11: Results of group ANOVA test for the yaw angle of the bees of different wingspan groups as they passed through the different gap treatments (Figure 3a). Details on Wingspan groups and Gapsize treatments is indicated in Table S1.

Supplementary Videos

SV1: Animation of the experiment setup with a cartoon of a bumblebee approaching a narrow gap and flying through it.

SV2: Representative video of a bumblebee with wingspan = 27.5mm encountering a 25mm wide gap. The bee scans the gap by performing lateral peering motion between the edges of the gap before passing through it by reorienting itself from increasing its yaw/heading angle. Some contact between the bee's antennae and legs with the edges of the gap can be noted. Upon passing through the gap the bees right themselves to realign with their flight direction.

SV3: Representative video of a bumblebee with wingspan = 26 mm encountering a 50 mm wide gap. The bee scans the gap by peering between the edges and traverses through it without any change in yaw angle.

SV4: Representative video of a bumblebee with wingspan = 25.6 mm encountering a 35 mm wide gap. The bee scans the gap by performing lateral peering motion between the edges of the gap before passing through it. Though the bee reorients itself by increasing its yaw angle, the reorientation is not as high as those noted when passing smaller gaps (SV2).

SV5: Representative close up video of a bumblebee of wingspan = 23 mm passing through a 20 mm wide gap. The bee reorients to safely pass through the gap. Some contact between the bee's antennae with the edges of the gap can also be noted.

SV6: Representative video of a bumblebee with wingspan = 26.8 mm encountering a 25 mm wide gap. The bee scans the gap by performing lateral peering motion between the edges of the gap before passing through it. Contact between the bee's antennae and legs with the edges of the gap can be noted.

SV7: Representative video of a bumblebee with wingspan = 26 mm encountering a 20 mm wide gap. The bee appears to head-butt the obstacle as it reorients itself and fly through the gap. The head-butt appears to be deliberate since leg extension reflex is not noted.

Dataset

Dataset file includes all data used to create Figures 2 & 3 of the main text. All data arranged in as separate pages. Number_of_Peering_Passes: data of number of peering passes performed by the bees of different sizes ahead of the different gaps. Peering_Amplitude: data of the amplitude the bees peered ahead of the different gaps. Peering_Time_vs_Gapsize: data of time bees of different size spent peering ahead of the gaps. Yaw_Angle_of_Bees_vs_Gapsize: data of the yaw or heading angle of the bees as they crossed the different gaps. %_of_Wing_Collision_with_Gap: data of the percent of time bees of different sizes collided with the gaps. %_of_Head&Body_Contact_with_Gap: data of the percent of time the bees' body or head made contact with the gap/

SI References

1. A. Werner, W. Stürzl, J. Zanker, Object recognition in flight: How do bees distinguish between 3D shapes? *PLoS One* **11** (2016).
2. S. Ravi, *et al.*, Gap perception in bumblebees. *J. Exp. Biol.* **222** (2019).
3. M. Egelhaaf, N. Boeddeker, R. Kern, R. Kurtz, J. P. Lindemann, Spatial vision in insects is facilitated by shaping the dynamics of visual input through behavioral action. *Front. Neural Circuits* **6**, 108 (2012).
4. M. V Srinivasan, S. W. Zhang, Visual control of honeybee flight. *EXS* **84**, 95–113 (1997).
5. D. Floreano, J. C. Zufferey, M. V. Srinivasan, C. Ellington, *Flying Insects and Robots*, D. Floreano, J.-C. Zufferey, M. V. Srinivasan, C. Ellington, Eds. (Springer Berlin Heidelberg, 2010) https:/doi.org/10.1007/978-3-540-89393-6.
6. M. V. Srinivasan, M. Lehrer, Temporal acuity of honeybee vision: behavioural studies using moving stimuli. *J. Comp. Physiol. A* **155**, 297–312 (1984).
7. F. T. Muijres, M. J. Elzinga, J. M. Melis, M. H. Dickinson, Flies evade looming targets by executing rapid visually directed banked turns. *Science* **344**, 172–7 (2014).
8. S. Ravi, *et al.*, Bumblebees minimize control challenges by combining active and passive modes in unsteady winds. *Sci. Rep.* **6**, 35043 (2016).
9. G. K. Taylor, Mechanics and aerodynamics of insect flight control. *Biol. Rev. Camb. Philos. Soc.* **76**, 449–471 (2001).
10. S. Ravi, *et al.*, Bumblebees minimize control challenges by combining active and passive modes in unsteady winds. *Sci. Rep.* **6** (2016).
11. F. van Breugel, K. Morgansen, M. H. Dickinson, Monocular distance estimation from optic flow during active landing maneuvers. *Bioinspir. Biomim.* **9**, 025002 (2014).
12. J. R. Serres, F. Ruffier, Optic flow-based collision-free strategies: From insects to robots. *Arthropod Struct. Dev.* **46**, 703–717 (2017).
13. O. J. N. Bertrand, J. P. Lindemann, M. Egelhaaf, A Bio-inspired Collision Avoidance Model Based on Spatial Information Derived from Motion Detectors Leads to Common Routes. *PLOS Comput. Biol.* **11**, e1004339 (2015).
14. J. J. Gibson, P. Olum, F. Rosenblatt, Parallax and perspective during aircraft landings. *Am. J. Psychol.* **68**, 372–85 (1955).
15. M. V Srinivasan, Honey bees as a model for vision, perception, and cognition. *Annu. Rev. Entomol.* **55**, 267–84 (2010).
16. J. Hateren, C. Schilstra, Hateren, Schilstra, Blowfly flight and optic flow. II. Head movements during flight. *J. Exp. Biol.* **202 (Pt 11**, 1491–500 (1999).
17. N. Boeddeker, J. M. Hemmi, Visual gaze control during peering flight manoeuvres in honeybees. *Proceedings. Biol. Sci.* **277**, 1209–17 (2010).
18. N. Boeddeker, *et al.*, The fine structure of honeybee head and body yaw movements in a homing task. *Proc. R. Soc. B Biol. Sci.* **277**, 1899–1906 (2010).
19. W. H. Warren, S. Whang, Visual guidance of walking through apertures: body-scaled information for affordances. *J. Exp. Psychol. Hum. Percept. Perform.* **13**, 371–83 (1987).
20. I. Schiffner, H. D. Vo, P. S. Bhagavatula, M. V Srinivasan, Minding the gap: in-flight body awareness in birds. *Front. Zool.* **11**, 64 (2014).
21. , The three-dimensional word of a toad. *Proc. R. Soc. London. Ser. B. Biol. Sci.* **206**, 481–487 (1980).